

# RSC Advances



This is an *Accepted Manuscript*, which has been through the Royal Society of Chemistry peer review process and has been accepted for publication.

*Accepted Manuscripts* are published online shortly after acceptance, before technical editing, formatting and proof reading. Using this free service, authors can make their results available to the community, in citable form, before we publish the edited article. This *Accepted Manuscript* will be replaced by the edited, formatted and paginated article as soon as this is available.

You can find more information about *Accepted Manuscripts* in the [Information for Authors](#).

Please note that technical editing may introduce minor changes to the text and/or graphics, which may alter content. The journal's standard [Terms & Conditions](#) and the [Ethical guidelines](#) still apply. In no event shall the Royal Society of Chemistry be held responsible for any errors or omissions in this *Accepted Manuscript* or any consequences arising from the use of any information it contains.

**Application of Cobalt oxide nanostructured modified aluminium electrode for electrocatalytic oxidation of Guanine and Single Strand DNA**

Vairamuthu Raj\*, Jayachandran Silambarasan, Panchanathan Rajakumar

*Advanced Materials Research Laboratory, Department of Chemistry, Periyar University, Salem-636 011, Tamil Nadu, India.*

*\*Corresponding author*

*Dr. V. Raj,*

*Department of Chemistry,*

*Periyar University,*

*Salem 636 011,*

*Tamil Nadu, INDIA.*

*Tel: 0427-2345271 Fax: 0427-2345124*

*E-mail address: [alaguraj2@rediffmail.com](mailto:alaguraj2@rediffmail.com)*

## Abstract

A novel electrochemical biosensor for the selective and sensitive determination of guanine and single strand DNA (ss-DNA) has been developed by electrodeposition of cobalt oxide nanoflowers (CoOx) on the aluminium electrode (Al). The modified aluminium electrode showed an excellent intensification of the guanine oxidation response in ss-DNA. The morphological characteristics, phase composition and electrochemical properties of the modified electrode were studied by SEM, XRD and Electrochemical Impedance Studies. The effects of scan rate, pH, and concentration of ss-DNA and guanine on the response of the sensor have been studied. The detection limits of 4 and 450 nM were obtained for guanine and ss-DNA, respectively. Simplicity of fabrication, excellent electrocatalytic ability, high stability and selectivity of the modified electrode have been achieved.

**Keywords:** Nanobiosensors, Aluminium electrode, Cobalt oxide nanoflowers, Electrodeposition, Guanine, Single Strand DNA.

## 1. Introduction

DNA analysis plays an ever-increasing role in a number of areas related to human health such as diagnosis of infectious diseases, genetic mutations, drug discovery, forensics and food technology. For this study, this conclusion, a number of assay techniques are available, but primarily, sequencing is achieved through tagging of a DNA sample with a fluorescent compound<sup>1</sup>. As an option, the use of electrochemistry may provide a cheaper and more cost-effective method of DNA assay. Both purine bases (guanine and adenine) are of special interest to electrochemistry due to the relative ease with which they may be oxidized and thus allow

quantification of a DNA sample. Guanine is an important component found in DNA and is the most readily oxidized form of the four nucleic acid bases<sup>2-4</sup>. It is believed that guanine frolicked a key role in the oxidation of DNA by various types of oxidants and free radicals.

Semiconductor nanostructures<sup>5,6</sup> especially metal oxide nanostructures, with unique properties and applications in many areas, configured as electronic devices have come forth as a universal program for ultra-sensitive direct electrical detection of biological and chemical species. Sensing behavior is one of the most important and well-known properties of metal oxide sensors, which usually demonstrates much higher sensitivity to their chemical environment than the other chemical/biosensors in their sensitivity, selectivity and stability. The sensing mechanism of metal oxide materials is primarily regulated by the fact that the oxygen vacancies on the oxide surfaces are electrically and chemically active. In this example, two sorts of sensing responses have been observed<sup>7, 8</sup>. First, electrons in metal oxides are withdrawn and effectively depleted from the conduction band upon adsorption of charge accepting molecules, such as NO<sub>2</sub> and O<sub>2</sub>, at the vacant sites, leading to a reduction of conductivity. On the other hand, in an oxygen-rich environment, chemical molecules such as CO and H<sub>2</sub> react with the surface adsorbed oxygen and therefore release the captured electrons back to the channel, resulting in an increase in metal oxides conductance.

Cobalt oxides (CoOx) are versatile materials for emerging fields, such as clean energy, biomaterials, and catalysis<sup>9</sup>. Nanostructured cobalt oxide hydroxide (CoOOH) and Co<sub>3</sub>O<sub>4</sub> materials have remarkable electrochemical properties for applications in batteries, fuel cells, sensors, and others<sup>10-12</sup> due to their excellent electrocatalytic activity. For many of these applications, high surface area and conductivities of materials are crucial. Electrodeposition as a

simple and easy procedure method for fabrication of CoOx films is very interesting<sup>13, 14</sup>. Lately, various forms of cobalt oxide nanomaterials have been applied to construct chemical sensors or biosensors based on the electrocatalytic ability of the cobalt oxide redox couple for oxidation processes. Electrocatalytic oxidation of hydrogen peroxide<sup>15</sup>, hydroquinone<sup>16</sup>, glutathione<sup>17</sup>, glucose<sup>18</sup> and arsenic<sup>19</sup> on electrodeposited CoOx nanostructures on various electrodes. Owing to biocompatibility of cobalt oxide nanostructures, the proposed nanomaterials have also been used to immobilize biomolecules such as FAD, cholesterol oxidase and hemoglobin<sup>20-22</sup>.

Until today, the widely used electrode for determination of guanine are glassy carbon<sup>23</sup>, and carbon paste electrodes<sup>24</sup>. Aluminium is the cheapest metal possessing unique properties such as excellent thermal and electrical conductivity, low density, lightweight, etc. By changing the surface of aluminium<sup>25, 26</sup>, an assortment of novel sensors can be constructed, which can compete even with carbon nanotube (CNT) modified electrodes.

Based on the comprehensive literature, it was found that no work has been reported on fabrication of chemical or electrochemical sensor using Al electrode deposited with CoOx nanoflowers for the detection of biomolecules. For the first time, we are reporting here the mechanistic studies on the electrocatalytic oxidation of guanine and single-strand DNA (ss-DNA) with a simply prepared cobalt oxide nanostructure modified aluminium electrode. The probable analytical application of the modified electrode was assessed, and it has been used for voltammetric detection of guanine in the nanomolar concentration range. The present study expands the application range of cobalt oxide nanomaterials into the detection of important biomolecules using an electrochemical method.

## 2. Experimental

## 2.1. Reagents

Guanine and Double-stranded DNA (dsDNA) from the calf thymus were obtained from Sigma. Cobalt (II) nitrate, sodium nitrate and potassium chloride, potassium hexacyanoferrate and all other reagents were obtained from Merck, India and used without further purification. Double distilled, deionized water was applied throughout the study. A  $5 \mu\text{g mL}^{-1}$  solution of guanine was prepared daily by dissolving appropriate amounts of guanine in 100 ml of alkali media (NaOH 0.1 M). This solution was diluted to the appropriate concentration, and its pH was adjusted by the addition of acetic acid.

## 2.2. Preparation of ss-DNA samples

Thermally denatured dsDNA was produced according to the previous report<sup>27</sup>. In short native calf thymus dsDNA samples were dissolved in water, and then the solution was heated in a boiling-water bath (100 °C) for about 10 min. Finally, the solution was rapidly cooled in an ice bath. Generally, thermal denaturation involves the rupture of hydrogen bonds, the disturbance of stacking interaction, but not any breakage of a covalent bond. So, thermally denatured dsDNA may act as ss-DNA. The obtained solution was diluted to an appropriate concentration daily using phosphate buffer solution (pH 7.2).

## 2.3. Modified electrode fabrication

An aluminium sheet (purity 99.99%, thickness 0.3 mm) was used as a substrate for the preparation of CoOx nanoflowers. Before electrodeposition, the aluminium was annealed at 450°C for a half an hour, and it was etched in 5% sodium hydroxide for 2 min to remove the native barrier layer and followed by rinsing in distilled water. After etching, the electrode was

rinsed in distilled water. Then the Al electrode was chemically polished with a mixture of concentrated sulphuric, nitric and phosphoric acids. Prior to electrodeposition, electrode was dipped in phosphoric acid for 5 min to bump off the oxide layer.

#### **2.4. Formulation and Characterization of CoOx Array Films**

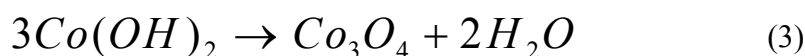
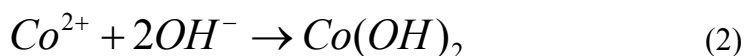
The electrodeposition of cobalt oxide was performed in a standard three-electrode glass cell at 20 °C, using the aluminium electrode as working electrode, a saturated calomel electrode (SCE) as the reference electrode and Pt foil as a counter electrode. The precursor films<sup>28</sup> were electrodeposited from aqueous solution containing 0.6 M Co(NO<sub>3</sub>)<sub>2</sub> and 0.05 M NaNO<sub>3</sub> using a CHI 760c Electrochemical Workstation. The electrodeposition experiment was carried out at a constant potential of -1.0 V Vs calomel electrode for various times. After the electrochemical deposition, the electrode was washed with deionized-water, dried at 85 °C and then annealed at 250°C in air for 1 h in order to transform Co(OH)<sub>2</sub> into Co<sub>3</sub>O<sub>4</sub>.

#### **2.5. Instrumentation**

The electrodeposition of the CoOx Nanoflowers and electrochemical measurements were done with a CHI 760C electrochemical workstation (CH Instrument Inc., USA). Voltammetric experiments were taken out utilizing a schematic three-electrode system with aluminium having a diameter of 3.0 mm as the working electrode, a Pt coil as the auxiliary electrode, and calomel as the reference electrode. A Hitachi SU-70 was employed for Field Emission Scanning Electron Microscopy (FE-SEM) and X-ray diffraction (XRD) experiments. All experiments were done at room temperature.

### **3. Results and discussion**

The formation of CoOx nanoflowers on the aluminium electrode by electrodeposition may involve the following mechanism. The electrodeposition process of the Co(OH)<sub>2</sub> precursor film would include an electrochemical reaction, precipitation and followed by annealing can be stated as<sup>29</sup>,



### 3.1 SEM and XRD pattern of CoOx/Al

**Figure 1** shows the SEM image of a typical sample composed of many uniform flower like architectures approximately 500 nm in diameter. The detailed morphology of CoOx/Al is shown in Figure 1b, which reveal that the full construction of the nanoflowers is built from several dozen nanopetals with smooth surfaces. These nanopetals are connected to each other through the center to form 3D flower like structures. The figure also shows that the petals are porous because of the removal of water molecules at high temperature<sup>30</sup>. In that morphology, triangular shaped porous structures are also found, which are formed by merging of approximately three or four nanopetals (inset **fig. 1(b)**). This triangular shaped porous CoOx nanoflowers placed in different angles have high surface area and easily pulls the particles from the environment, which forms a conduit to exchange electrons.

The surface of the petals of the CoOx nanoflowers are very smooth, probably due to Ostwald ripening. The morphology of the CoOx nanoflower depends on several factors,



including crystal-face attraction, electrostatic and dipolar fields associated with the aggregate<sup>31</sup>, Vander Waals forces<sup>32</sup>, hydrophobic interactions<sup>33</sup>, and hydrogen bonds<sup>34</sup>.

The XRD pattern of as-deposited CoOx nanoflowers on the aluminium electrode is shown in **Fig. 1(c)**. The diffraction peaks of the CoOx nanoflowers can be indexed as the spinel cubic Co<sub>3</sub>O<sub>4</sub> phase (JCPDS No. 42-1467) indicating that, which means that the precursor Co(OH)<sub>2</sub> transformed into the Co<sub>3</sub>O<sub>4</sub> nanoflower. The sharp peaks conform the polycrystalline nature of the CoOx nanoflower.

### 3.2. Electrochemical characterization of the modified electrodes

Electrochemical impedance spectroscopy (EIS) provides detailed information on the change of the surface property of modified electrodes. The impedance spectra includes a semicircle portion and a linear portion. The semicircle diameter at higher frequencies corresponds to the electron transfer limited process or electron-transfer resistance ( $R_{et}$ ), and this resistance controlled the electron transfer kinetic process of the redox probe on the electrode interface. The linear portion at lower frequencies corresponds to the diffusion process. The typical Nyquist diagrams of equivalent [Fe(CN)<sub>6</sub>]<sup>3-/4-</sup> at the bare Al and CoOx/Al electrodes are illustrated in **Fig. 2**. The  $R_{et}$  of the bare Al electrode is estimated to be 994  $\Omega\text{ cm}^{-2}$ . Later, a further decrease of the  $R_{et}$  (519  $\Omega\text{ cm}^{-2}$ ) is observed due to the electrodeposition of the CoOx nanoflowers, implying that the presence of CoOx nanoflowers plays a significant part in accelerating the transfer of the electrons, thus decreasing the resistance of the CoOx/Al to Fe(CN)<sub>6</sub><sup>4-/3-</sup>. These effects indicate that CoOx nanoflowers was modified successfully on the surface of aluminium and greatly enhanced the conductivity.

### 3.3. Electrocatalytic oxidation of Guanine and ss-DNA at the Surface of CoOx/Al – modified electrode aluminium electrode

The electrochemical reduction and oxidation of natural nucleic acids are irreversible and occur at highly negative and positive potentials, respectively. The oxidation of guanine is irreversible and take place at highly positive potential at conventional electrodes. This nucleic acid roughly shows an oxidation peak at 0.9 – 1.0 V at the different surface electrodes<sup>35-37</sup>. Since the oxidation peak of guanine is close to a well-defined oxidation peak of CoOx that appears in the phosphate buffer medium, therefore, we expected an electrocatalytic mechanism initiated by electrochemical oxidation of the reduced form of the CoOx exist at the surface of the electrode and then completed by chemical oxidation of guanine, which also serves to regenerate the reduced form of the CoOx; so this system can be used for electrocatalytic oxidation of guanine. To exhibit the electrocatalytic activity of CoOx nanoflowers toward the oxidation of guanine, the voltammetric behavior of guanine was investigated at the surface of bare and CoOx-modified aluminium electrode. Fig. 3. (A) shows the cyclic voltammograms of CoOx nanoflowers – modified aluminium electrode in a 0.25 M phosphate buffer solution in the absence (curve a) and in the presence (curve b) of 0.5  $\mu$ M guanine. As shown, for the CoOx/Al electrode (curve a), a low redox response obtained in the absence of guanine can be seen in the potential range 0.5 to 1.1 V. After addition of guanine at the CoOx/Al electrode (curve b), the oxidation current of cobalt oxide nanoflowers was greatly increased due to the electrocatalytic oxidation of guanine. Similar results were obtained via the oxidation of ss-DNA that is shown in Fig. 3B. In this figure again, cyclic voltammogram indicates the signal of the CoOx-modified aluminium electrode in 0.25 M phosphate buffer solution, Fig.3B shows the cyclic voltammogram related to 25  $\mu$ M ss-DNA (the signal of 25  $\mu$ M ss-DNA on the surface of the bare electrode was subtracted). The

anodic peak current of the CoOx/Al increased due to the presence of guanine or ss-DNA, whereas cathodic peak current of this CoOx decreased accordingly. The anodic peak potential for the oxidation of guanine at CoOx modified aluminium electrode is about 0.791 V. Therefore, an enhancement of peak current is achieved in this system, which clearly demonstrates the occurrence of an electrocatalytic process. As shown in Fig.3, for the bare Al electrode (curve c), has no significant redox response obtained in the electrocatalytic oxidation of guanine and ss-DNA.

### 3.4 Effect of CoOx deposition time on electrocatalytic property of CoOx/Al electrode

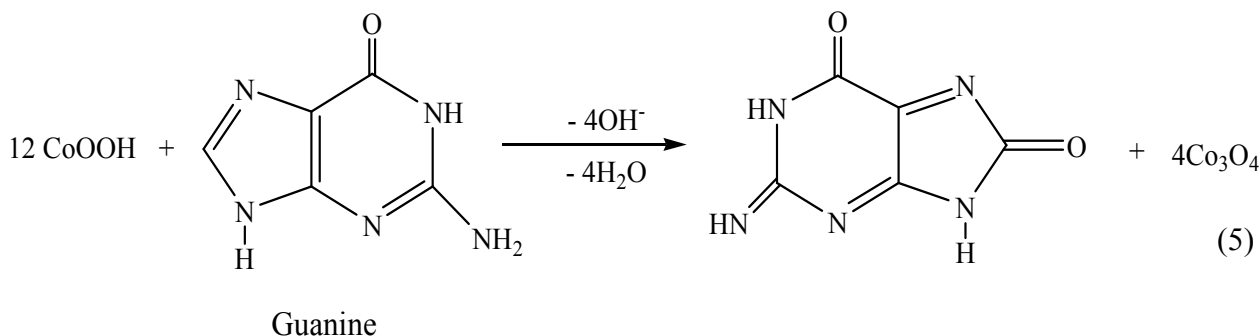
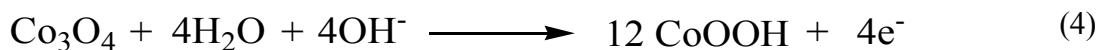
The film thickness of the porous thin film modified electrode disturbs both kinetics of the electrode processes and mass transfer mechanism via diffusion through the porous film<sup>38-41</sup> and thus, has a predominant role in the voltammetric response of these electrodes toward different analytes. The electrodeposition technique was chosen to produce the thin, porous films of CoOx nanoflowers on Al electrode surface as the layer thickness may be easily moderated. The attained result of the amount of deposited CoOx nanoflowers on the response current was investigated and the corresponding results are shown in **Fig. 4**. The response current of the CoOx/Al to the addition of 1  $\mu\text{M}$  guanine increased with the duration of the CoOx deposition time from two to four minutes, showing that the modification of the Al with thin films of CoOx nanoflowers results in a significant intensification of the guanine oxidation response. However, when the CoOx deposition time is more than four minutes, the response current decreased. This might be linked with a decrease in the actual “working” surface area of the electrode that results from excess deposition when larger volumes of CoOx nanoflowers might be aggregated on the electrode surface. In light of this possibility, the deposition time of four minutes was thus chosen for further sensor optimization and study.

### 3.5. Effect of pH

In order to assess the optimum pH and to evaluate the ratio of electrons and protons involved in the anodic oxidation of guanine on the surface of the modified electrode, the experiments were carried out at various pH. Accordingly, as shown in **fig. 5**, the electrocatalytic activity of the modified electrode toward guanine oxidation is pH dependent. In the pH range 12–5, the modified electrode shows electrocatalytic activity, but higher peak currents are observed at pH 6. This pH was selected as a most auspicious value for determining the experiments. Additionally, peak potentials are shifted to higher positive potentials with decreasing pH values and no peak current was observed at pH values below 4, due to the disintegration of the cobalt oxide film. As illustrated, both peak current and potentials are dependent on pH values of buffer solution.

### 3.6. Kinetics of electrocatalytic oxidation of guanine on modified electrode

**Fig. 6a** shows the cyclic voltammograms of 0.5  $\mu\text{M}$  guanine solution at different scan rates. The peak current ( $I_p$ ) for anodic oxidation of guanine is proportional to the square root ( $v^{1/2}$ ) of the scan rate (**Fig. 6b**) proposing that the process is controlled by diffusion of analyte as expected for a catalytic system. It can likewise be noted in **Fig. 6c** that by cumulative the scan rate, the peak potential for the catalytic oxidation of guanine moves to more positive values and the plot of peak current vs square root of scan rate deviates from linearity (at  $v > 200 \text{ mVs}^{-1}$ ), suggesting a kinetic limitation in the reaction between the redox sites of the cobalt oxide nanostructures and guanine. Established on the findings, the following catalytic framework describes the reaction sequence in the oxidation of guanine by the cobalt-oxide nanostructures, which is comparable to those reported previously<sup>42, 43</sup>.



A plot of  $\log I$  versus  $\eta$  (overpotential), recognized as Tafel plot, is a useful device for evaluating kinetic parameters<sup>44</sup>. The Tafel slope can be obtained by the method according to the following equation valid for a totally irreversible diffusion controlled process<sup>45</sup>.

$$E_p = \frac{b}{2} \log v + a \quad (6)$$

On the basis of this equation, the slope of the  $E_p$  versus  $\log v$  plot (**Fig. 6c**) is  $b/2 = \partial E_p / \partial \log v$ , where  $b$  indicates the Tafel slope. So,  $b = 2 \times 58 = 116 \text{ mV/s}$ . This slope yields a value of 2.71 for  $(1-\alpha)n_a$  which indicate a one-electron transfer to be the rate limiting step, assuming a transfer coefficient of  $\alpha = 0.3$ .

The number of electrons in the overall reaction ( $n$ ) can also be obtained from the slope of  $I_p$  vs  $v^{1/2}$  according to the following equation<sup>46</sup>,

$$I_p = 2.99 \times 10^5 n [n_a (1-\alpha)]^{1/2} A C_s D^{1/2} v^{1/2} \quad (7)$$

where  $\alpha$  is the charge transfer coefficient (calculated from the Tafel slope) and all other symbols have their conventional meaning. The total number of electrons involved in the anodic oxidation of guanine is 3.79. The four electron transfer in the oxidation of guanine at other modified electrodes was reported<sup>42, 43 & 36</sup>.

### 3.7. Analytical application

The DPV technique is one of the most sensitive and high resolution techniques compared to the CV technique in order to examine the electrochemical behavior of reactant molecules which are bound to the electrode surface. **Fig. 7a** displays the different concentrations of guanine ranging from 50 nM - 10  $\mu$ M at CoOx-modified Al electrode that were obtained by the Differential Pulse Voltammetry (DPV). As can be seen in **fig. 7b** the linear dynamic range for guanine is  $I_{pa} (\mu A) = 0.53 C_{\text{guanine}} (\text{nM}) + 101.54$  ( $R^2 = 0.995$ ). Deviation from linearity was observed for more concentrated solutions, due to the adsorption of guanine or its oxidation product on the electrode surface. By using  $3S_b$  in the calibration equation, we have calculated the detection limit concentration. The detection limit of 4 nM and sensitivity of 0.53  $\mu A/\mu M$  were achieved.

The pertinence of the modified electrode in biological samples was assessed by measuring guanine in ss-DNA of calf thymus. **Fig. 8a** shows the DPV of various concentrations of ss-DNA, ranging from 5 - 55  $\mu$ M in PBS (pH 6). As can be seen, the acid-denatured ss-DNA gives well-defined peak due to the oxidation of guanine residue. In **fig. 8b** shows, the linear dynamic range for guanine is  $I_{pa} (\mu A) = 2 C_{\text{ss-DNA}} (\mu M) + 101.54$ . To determine the detection limit for DNA, the above procedure was performed but at the peak potential of DNA and the detection limit of 450 nM (based on  $3s_b$ ) and the sensitivity of 2  $\mu A/\mu M$  was estimated for ss-DNA. The detection limit, the linear calibration range and sensitivity of modified electrode for guanine detection are comparable and even improved than those received by using another modified electrodes (Table 1).

After each measurement the modified electrode was washed thoroughly with distilled water. The reproducibility of CoOx/Al electrode was estimated by comparing the oxidation peak current obtained for 10 determinations on a  $5 \times 10^{-6}$  mol L<sup>-1</sup> guanine solution at pH = 6. The relative standard deviation (RSD) of 3.2% (n = 10) revealed a good reproducibility of the method. Storage stability is a vital parameter for the assessment of the performance of the sensor, which was occasionally tested over 90% of its initial value after 45 days

### 3.8. Interference study and selectivity

**Figure 9** shows the electrocatalytic oxidation of guanine in ss-DNA at cobalt oxide nanostructure modified aluminium electrode. Selective detection of guanine in the presence of several interfering compounds potentially existing in biological liquids is a very advantageous feature for modified electrodes. To make evident the selectivity of the proposed electrochemical sensor, the interferences of different compounds were examined during DPV response for guanine. In the present work, **Fig. 10a** shows the interference effects of 1 mM ascorbic acid (AA), 0.5 mM uric acid (UA), 1  $\mu$ M dopamine (DP) and **Fig. 10b** shows other purine bases like adenine, thymine, and cytosine were tested on the DPV response of 1  $\mu$ M guanine. No adjustments in response current of guanine were observed in the presence of AA, UA, DP solutions or the mixtures of all. In the mixture of all these compounds by using the modified electrode, four well-defined waves with a very good resolution are resulted. Among these interferences, adenine, thymine and cytosine has no response, but AA, UA, and DP showed the oxidation process in the selected potential range. Consequently, this modified electrode can be utilized for detection of guanine in the presence of other themes. This may be due to the reason that guanine is the most easily oxidized base in DNA owing to its lowest potential<sup>47, 48</sup> and also it

tends to oxidized to form stable radical cations<sup>49</sup>. The attained results demonstrated the satisfactory selectivity of the proposed CoOx nanoflower modified Al electrode toward electrocatalytic oxidation of guanine at remarkable reduced over-voltage. Thus, the proposed electrode could be a practical sensor for determination of guanine in the assortment of various common oxidizable species without separation.

#### 4. Conclusions

In this paper, a porous and stable CoOx nanoflowers having high surface area obtained on Al electrode by electrodeposition and employed as biosensor toward the oxidation of guanine and ss-DNA in the phosphate buffer medium for the first time. We demonstrated that the well-defined oxidation peak potential of CoOx that appears in the phosphate buffer medium can electrocatalyze and improve dramatically the oxidation signal of guanine and ss-DNA. The relationship between current response and guanine concentration is linear in the concentration range 50 nM-10  $\mu$ M. The detection limit of guanine and ss-DNA are 4 nM and 450 nM, respectively. This modified electrode can be utilized as a sensitive and reproducible voltammetric sensor for guanine detection in a wide pH range at reduced overpotentials. The fabricated CoOx/Al not only exhibited strong catalytic oxidation activity on the way to guanine, but also providing selective detection even in the presence of other purine base. Furthermore, the modification procedure is simple and also Al electrode is less expensive compared to other electrodes and more expedient than those used for other guanine sensors. So our present study may present an alternative means for the creation of nanostructured modified aluminium electrode for the electrochemical detection of biomolecules.

#### Acknowledgements



One of the authors Jayachandran Silambarasan thanks the Council of Scientific & Industrial Research (CSIR), New Delhi, for the award of a Senior Research Fellowship (9/810 (0021)/2013-EMR-I) and UGC networking resource centre for providing visiting fellowship and Prof. T.P. Radhakrishnan, School of Chemistry, University of Hyderabad, India for providing facilities and counselling.

## References

- [1] J. Shendure, R.D. Mitra, C. Varma, G.M. Church, *Nat. Rev. Genet.*, 2004, **5**, 335-344.
- [2] C.L. Scott, M. Pumera, *Electrochem. Commun.*, 2011, **13**, 213-216.
- [3] A. Ferancova, S. Rengaraj, Y. Kim, J. Labuda, M. Sillanpaa, *Biosens. & Bioelectron.*, 2010, **26**, 314-320.
- [4] Y. Liu, D. Wang, J. Huang, H. Hou, T. You, *Electrochem. Commun.*, 2010, **12**, 1108-1111.
- [5] F. Patolsky, C.M. Lieber, *Materials Today.*, 2005, **8**, 20-28.
- [6] G.Z. Shen, Y. Bando, C.H. Ye, X.L. Yuan, T. Sekiguchi, D. Golberg, *Angew. Chem. Int. Ed.*, 2006, **45**, 7568-7572.
- [7] A. Kolmakov, Y.X. Zhang, G.Z. Cheng, M. Moskovits, *Adv. Mater.*, 2003, **15**, 997-1000.
- [8] C. Baratto, E. Comini, G. Faglia, G. Sberveglieri, M. Zha, A. Zappettini, *Sens & Actuators B Chem.*, 2005, **109**, 2-6.
- [9] Y. Liang, Y. Li, H. Wang, J. Zhou, J. Wang, T. Regier and H. Dai, *Nat. Mater.*, 2011, **10**, 780-786.
- [10] F. Cheng, J. Chen, *Chem. Soc. Rev.*, 2012, **41**, 2172-2192.
- [11] Y. Li, P. Hasin, Y. Wu, *Adv. Mater.*, 2010, **22**, 1926-1929.

- [12] Lian-Kui Wu, Ji-Ming Hu, *Electrochim. Acta.*, 2014, **116**, 158-163.
- [13] N. Spataru, C. Terashima, K. Tokuhiko, I. Sutanto, D. A. Tryk, S. M. Park, A. Fujishima, *J. Electrochem. Soc.*, 2003, **150**, E337-E341.
- [14] E. A. McNally, I. Zhitomirsky, D. S. Wilkinson, *Mater. Chem. Phys.*, 2005, **91**, 391-398.
- [15] A. Salimi, R. Hallaj, S. Soltanian and H. Mamkhezri, *Anal. Chim. Acta*, 2007, **594**, 24-31
- [16] L. F. Fan, X. Q. Wu, M. D. Guo and Y. T. Gao, *Electrochim. Acta*, 2007, **52**, 3654-3659.
- [17] Y. Hou, J. C. Ndamanisha, L. P. Guo, X. J. Peng and J. Bai, *Electrochim. Acta*, 2009, **54**, 6166 - 6171.
- [18] G. InnocenzoCasellaMaria Gatta, *J. Electroanal. Chem.*, 2002, **534**, 31 - 38.
- [19] A. Salimi, H. Mamkhezri, R. Hallaj and S. Soltanian, *Sens. Actuators, B*, 2008, **129**, 246 - 254.
- [20] A. Salimi, R. Hallaj and S. Soltanian, *Biophys. Chem.*, 2007, **130**, 122 - 131.
- [21] A. Salami, R. Hallaj, H. Mamkhezri and S. M. T. Hosaini, *J. Electroanal. Chem.*, 2008, **31**, 619–620.
- [22] A. Salimi, R. Hallaj and S. Soltanian, *Electroanalysis*, 2009, **21**, 2693 – 2700.
- [23] S. Chatterjee and A. Chen, *Electrochem. Commun.*, 2012, **20**, 29-32.
- [24] I. Balan, I.G.David, V. David, A. Stoica, C. Mihailciuc, I.Stamatin and A.A. Ciucu, *J. Electroanal. Chem.*, 2011, **654**, 8-12.
- [25] V. Raj, J. Silambarasan and P. Rajakumar, *J. Environ. Sci.* (in press) DOI: 10.1016/S1001-0742(13)60514-8

- [26] M.H. Pournaghi-Azar, F. Ahour and F. Pournaghi-Azar, *Sens. Actuators B: Chem.*, 2010, **145**, 334–339.
- [27] J. Marmur, R. Rownd and C.L. Schildkraut, Academic Press, New York, 1963, p. 232
- [28] X. H. Xia, J. P. Tu, J. Zhang, J. Y. Xiang, X. L. Wang, and X. B. Zhao, *ACS Appl. Mater. Interfaces.*, 2010, **2**, 186-192
- [29] W. Zhou, J. Zhang, T. Xue, D. Zhao and H. Li, *J. Mater. Chem.*, 2008, **18**, 905-910.
- [30] L.B. Kong, J.W. Lang, M. Liu, Y.C. Luo and L. Kang, *J. Power Sources.*, 2009, **194**, 1194-1201.
- [31] G. M. Whitesides and M. Boncheva, *Proc. Natl. Acad. Sci., USA.*, 2002, **99**, 4769-4774.
- [32] Y. Politi, T. Arad, E. Klein, S. Weiner and L. Addadi, *Science.*, 2004, **306**, 1161-1164.
- [33] H. Colfen and M. Antonietti, *Angew. Chem. Int. Ed.*, 2005, **44**, 5576- 5591.
- [34] H. Colfen and S. Mann, *Angew. Chem. Int. Ed.*, 2003, **42**, 2350-2355.
- [35] Z. Gao, *Sens. Actuators, B*, 2007, **123**, 293-298.
- [36] A. Abbaspour, L. Baramakeh and S. M. Nabavizadeh, *Electrochim. Acta*, 2007, **52**, 4798 – 4803.
- [37] J. Wang, J. R. Fernandes and L. T. Kubota, *Anal. Chem.*, 1998, **70**, 3699 - 3702.
- [38] I. Streeter, G.G. Wildgoose, L. Shao and R.G. Compton, *Sens. & Actuators. B: Chem.*, 2008, **133**, 462 – 466.
- [39] L. Xiao, G.G. Wildgoose and R.G. Compton, *Sens & Actuators B: Chem.*, 2009, **138**, 524-531.
- [40] M.C. Henstridge, *Sens. & Actuators B: Chem.*, 2010, **145**, 417–427.
- [41] G.P. Keeley and M.E.G. Lyons, *Inter. J. Electrochem. Sci.*, 2009, **4**, 794–809.

- [42] Z. Wang, S. Xiao and Y. Chen, *J. Electroanal. Chem.*, 2006, **589**, 237-242.
- [43] R. Hallaj and A. Salimi, *Analytical Methods.*, 2011, **3**, 911-918 .
- [44] A.J. Bard and L.R. Faulkner, John Wiley, New York, 2001
- [45] J.A. Harrison and Z.A. Khan, *J. electroanal. Chem* 1970., **28**, 131-138
- [46] S. Antoniadou, A. D. Jannakoudakis and E. Theodoridou, *Synth. Met.*, 1980, **30**, 295-304.
- [47] S. Steenken and S.V. Jovanovic, *J. Am. Chem. Soc.*, 1997 **119**, 617–618.
- [48] C.J. Burrows and J.G. Muller, *Chem. Rev.*, 1998, **98**, 1109-1152.
- [49] M. Tsoi, T.T. Do, V. J. Tang, J.A. Aguilera and Jamie R. Milligan. *Org. Biomol. Chem.*, 2010, **8**, 2553–2559
- [50] A. Abbaspour, M. Ayatollahi Mehrgardi and R. Kia, *J. Electroanal. Chem.*, 2004, **568**, 261-266.
- [51] A. Abbaspour, and M. Ayatollahi Mehrgardi, *Anal. Chem.*, 2004, **76**, 5690-5696.
- [52] H. Liu, G. Wang, D. Chena, W. Zhang, C. Li and B. Fang, *Sensors & Actuat B-Chem.*, 2008, **128**, 414-421.
- [53] F. Xiao, F. Zhao, J. Li, L. Liu and B. Zeng, *Electrochim. Acta.*, 2008, **53**, 7781-7788.

### Figure captions

**Table 1.** Analytical factor of different modified electrodes for guanine detection

**Fig. 1.** (A, B) Different magnifications of SEM image of CoOx/Al (C) XRD pattern image of CoOx nanostructure.

**Fig. 2.** Nyquist diagrams of (a) Bare aluminium, (b) CoOx/Al recorded in 5.0 mM  $[\text{Fe}(\text{CN})_6]^{3-/4-}$  containing 0.1 M KCl.

**Fig.3.** (A) Cyclic voltammograms of CoOx modified Al electrode (a) in the absence and (b) in the presence of 0.5  $\mu\text{M}$  guanine in 0.25 M phosphate buffer solution. (B) Cyclic voltammograms of CoOx modified Al electrode (a) in the absence and (b) in the presence of 25  $\mu\text{M}$  ss-DNA guanine in 0.25 M phosphate buffer solution. (c) Cyclic voltammogram of 0.5  $\mu\text{M}$  and 25  $\mu\text{M}$  ss-DNA guanine at the surface of the bare Al electrode, scan rate of  $100 \text{ mVs}^{-1}$  in 0.25 M phosphate buffer solution.

**Fig. 4.** Effect of electrodeposition time of CoOx/Al on peak current in the presence of 0.5  $\mu\text{M}$  guanine.

**Fig. 5.** Effect of pH on peak potential and peak current of the CoOx/Al-modified electrode in 0.25 M phosphate buffer solution containing 0.5  $\mu\text{M}$  guanine

**Fig. 6.** (a) Cyclic voltammograms of the CoOx/Al-modified electrode in 0.25 M phosphate buffer solution (pH 6) containing 0.5  $\mu\text{M}$  guanine at scan rates of 10-100  $\text{mV s}^{-1}$ . (b) Plot of anodic peak current vs square root of scan rate. (c) Plot of anodic peak potential vs  $\log v$ .

**Fig. 7.** DPV of various concentrations of (a) free guanine over the range of 50 nM-10  $\mu\text{M}$  in 0.25 M phosphate buffer solution. Pulse amplitude: 0.05V. Pulse width: 0.05s. Pulse period: 0.2s. (b) Calibration curve obtained from these voltammogram.

**Fig. 8.** DPV of various concentrations of (a) guanine in ss-DNA over range of 5-65  $\mu\text{M}$  in 0.25 M phosphate buffer solution. (b) Calibration curve obtained from these voltammogram.

**Fig. 9.** Graphical representation of electrocatalytic oxidation of guanine in ss-DNA at cobalt oxide nanostructure modified aluminium electrode

**Fig. 10.** (a) DPV for the determination of 0.6  $\mu\text{M}$  guanine in 0.25 M PBS (pH 7) at CoOx/Al in the presence of other purine base adenine (A -  $\blacklozenge$  curve), thymine (T -  $\bullet$  curve), cytosine (C -  $\blacksquare$

curve). (b) DPV for the determination of 0.6  $\mu\text{M}$  guanine ( $\bullet$ ) in 0.25 M PBS (pH 7) at CoOx/Al in the presence of 1 mM AA ( $\blacksquare$  curve), 0.1 mM UA ( $\blacktriangle$  curve), 10 $\mu\text{M}$  DP ( $\blacklozenge$  curve).

**Table 1** Analytical factors of different modified electrodes for guanine detection

Electrode	Analytical Method	Selectivity	E(V)	Linear dynamic range	Detection Limit (nM)
Redox polymer-modified indium tin oxide <sup>35</sup>	Amperometry	Guanine	0.65	8.0 nM–100 $\mu$ M	5.0
Cobalt(II) phthalocyanine modified carbon paste electrode <sup>50</sup>	DPV <sup>a</sup>	Guanine	0.920	----	550
$\beta$ -Cyclodextrin incorporated carbon nanotube-modified electrode <sup>42</sup>	DPV	Adenine and Guanine	0.79	200 nM–20 mM	200
Cobalt hexacyanoferrate modified carbon paste electrode <sup>51</sup>	Cv <sup>b</sup>	Guanine	0.9	0 – 4 $\mu$ g mL <sup>-1</sup>	340
Polythionine/Au-nanoparticles/MWCNT <sup>d</sup> modified electrode <sup>52</sup>	DPV	Adenine and Guanine	0.7	50 nM–5 mM	10
Ionic liquid/carbon nanotube/Au nanoparticle composite film <sup>53</sup>	DPV	Adenine and Guanine	0.7	8 nM–2 mM	5
Nanostructured platinum modified Glassy Carbon Electrode <sup>23</sup>	SWV <sup>c</sup>	Guanine	0.82	0.1 – 500 $\mu$ M	31

<b>Cobalt oxide nanostructure modified aluminium electrode (present study)</b>	DPV	Guanine	0.79	50 nM-10 $\mu$ M	4
<b><sup>a</sup>Differential Pulse Voltammetry, <sup>b</sup>Cyclic Voltammetry, <sup>c</sup>Square wave voltammetry, <sup>d</sup>Multi-Walled Carbon Nanotube.</b>					





Fig. 1

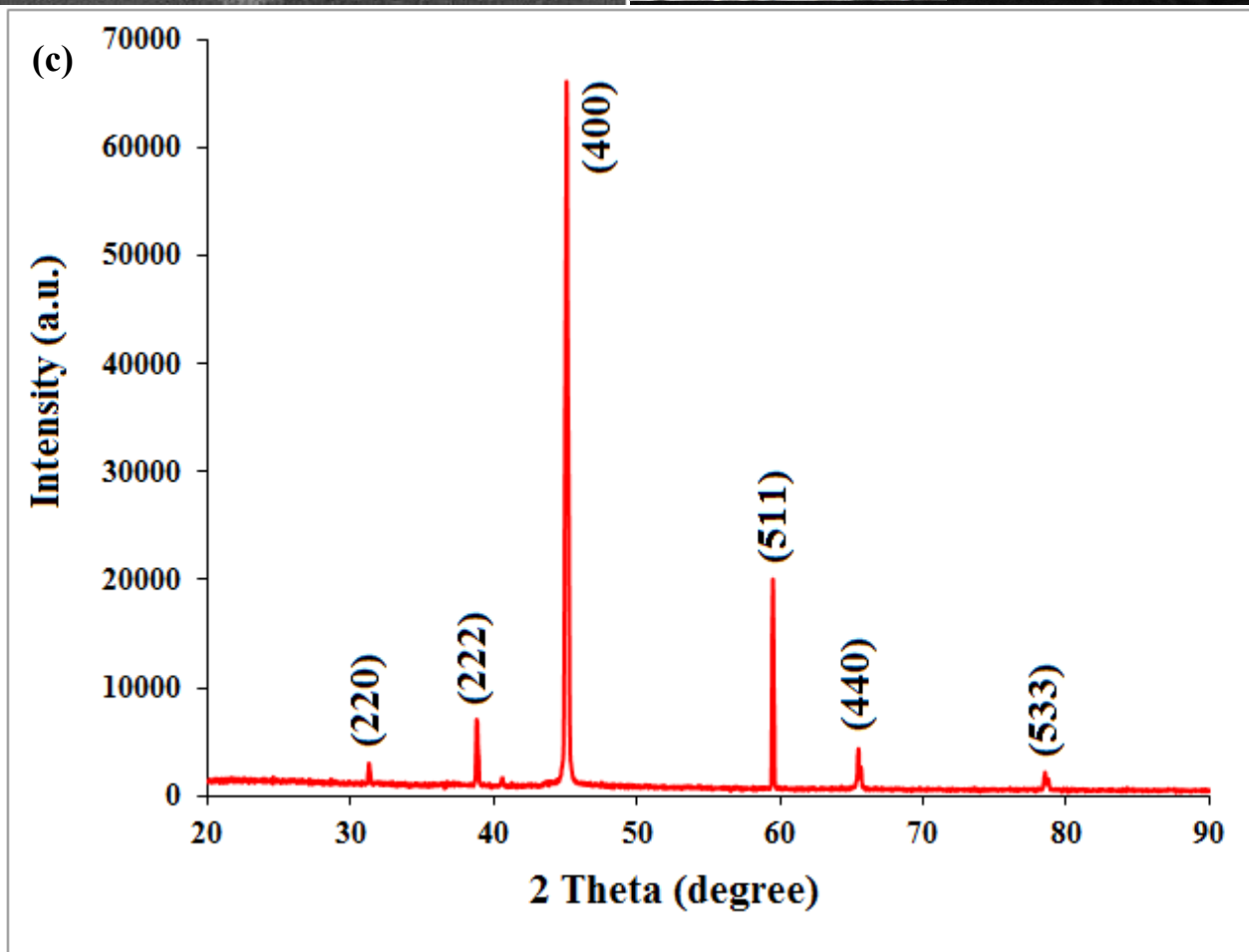
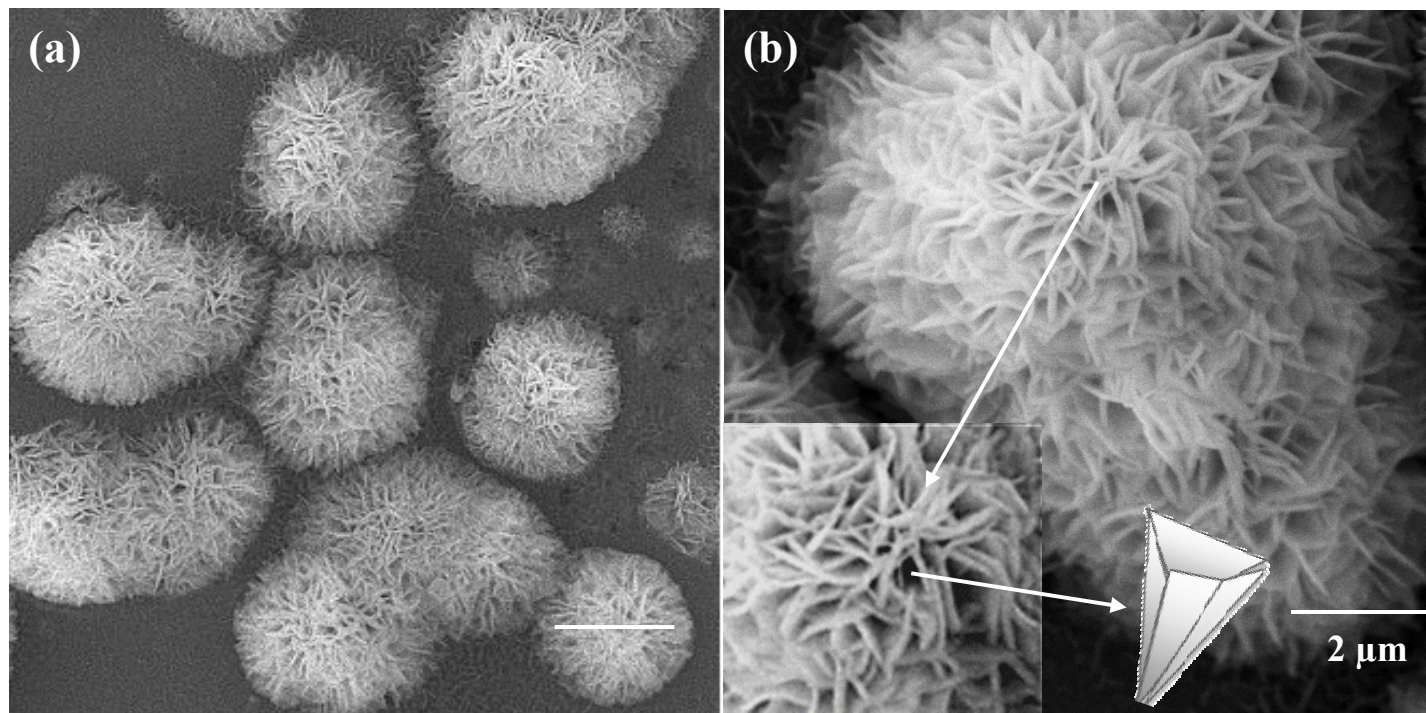


Fig. 2.

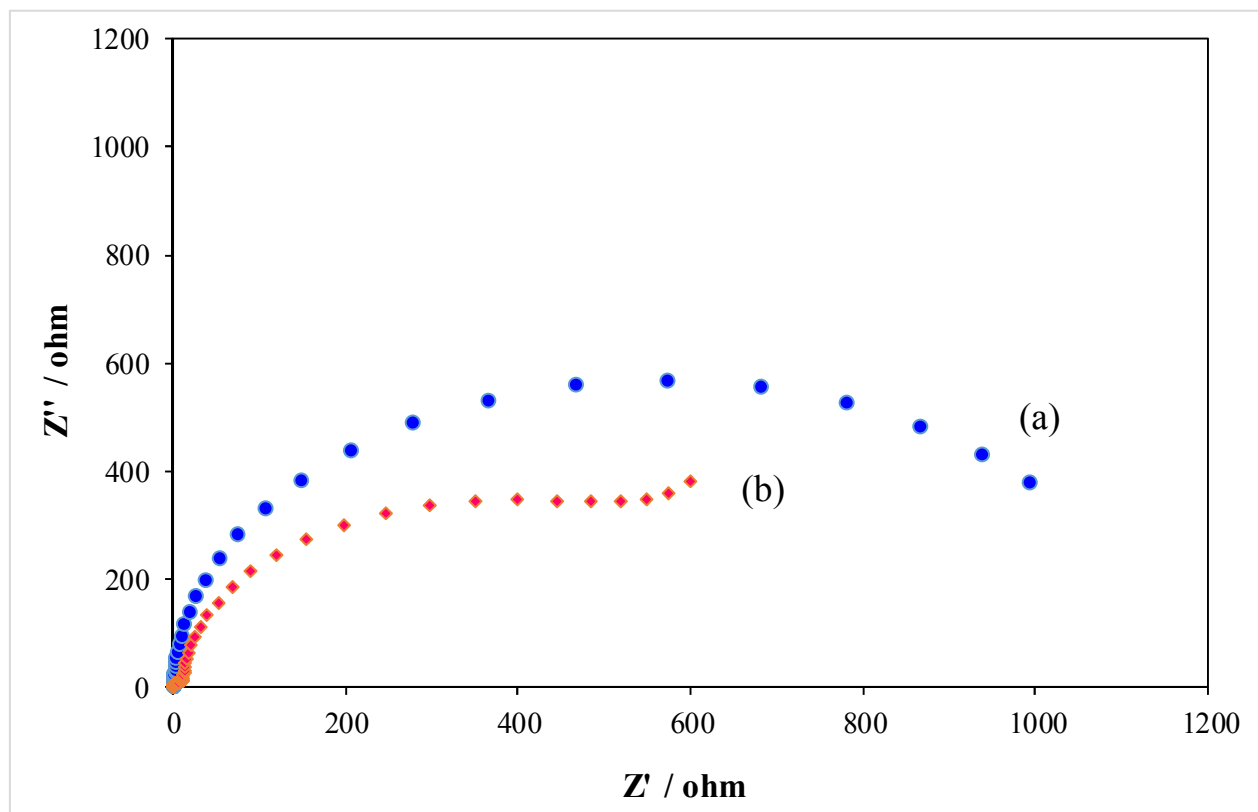


Fig. 3.

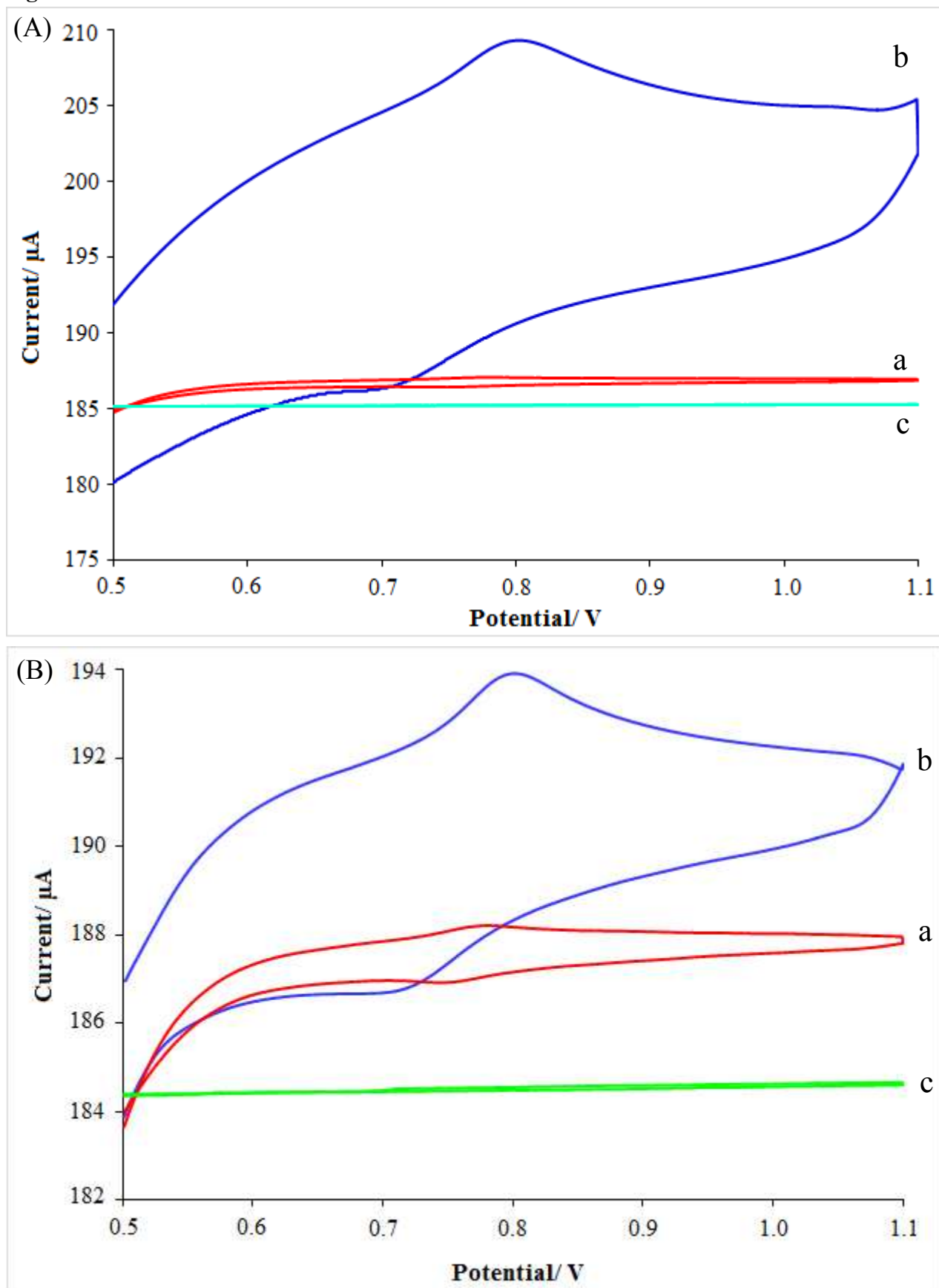


Fig. 4.

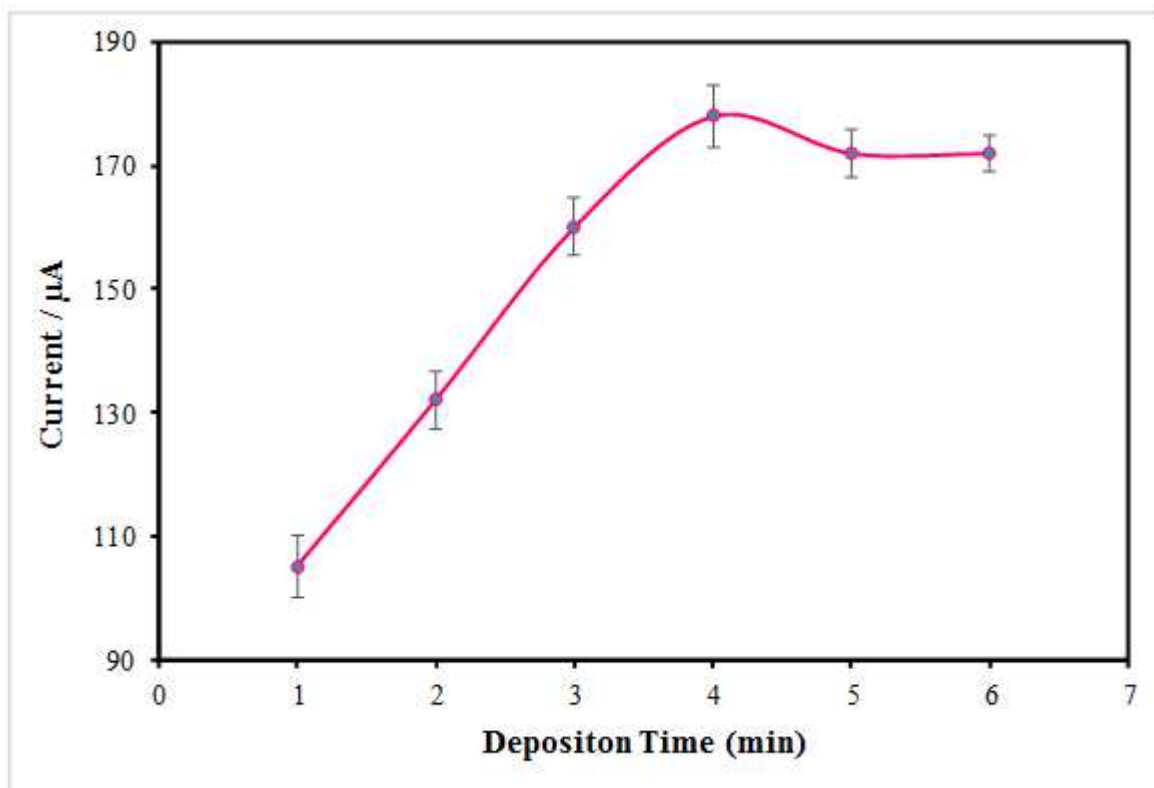


Fig. 5.

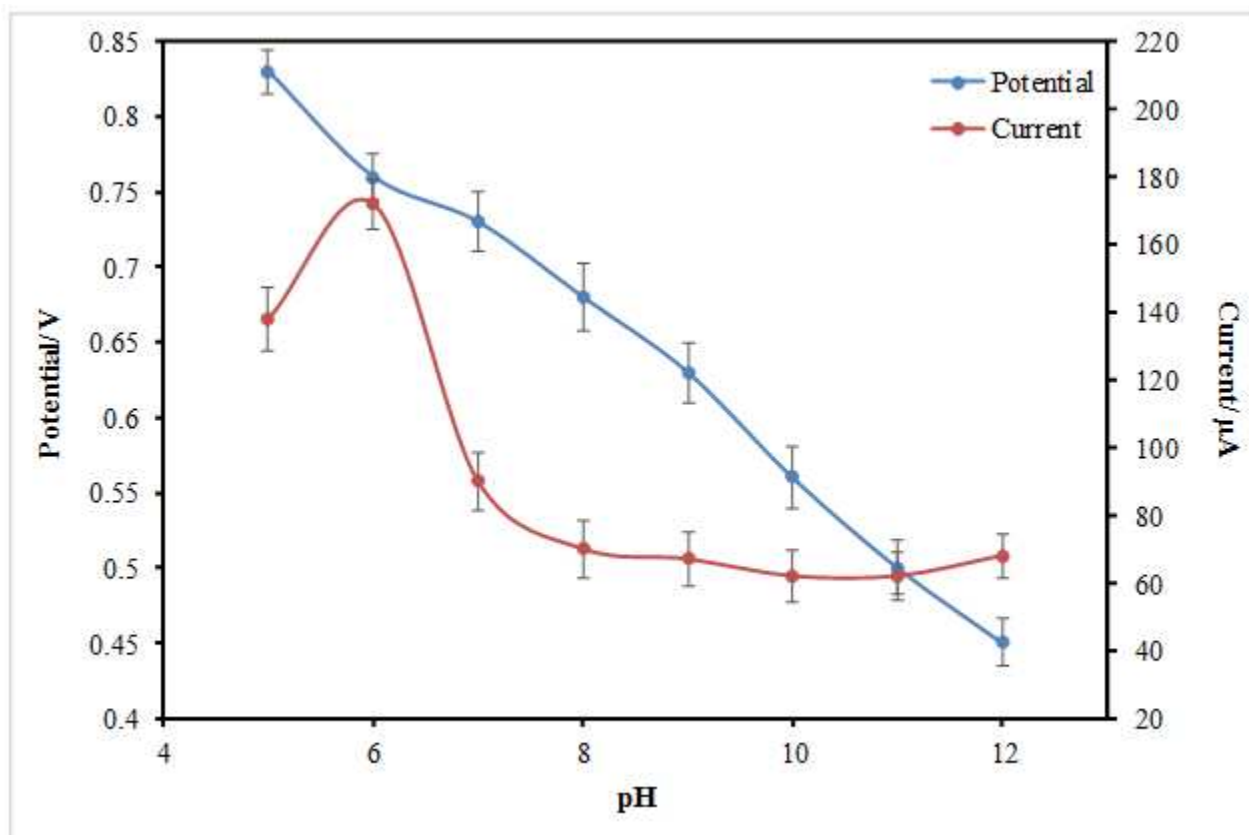


Fig. 6.

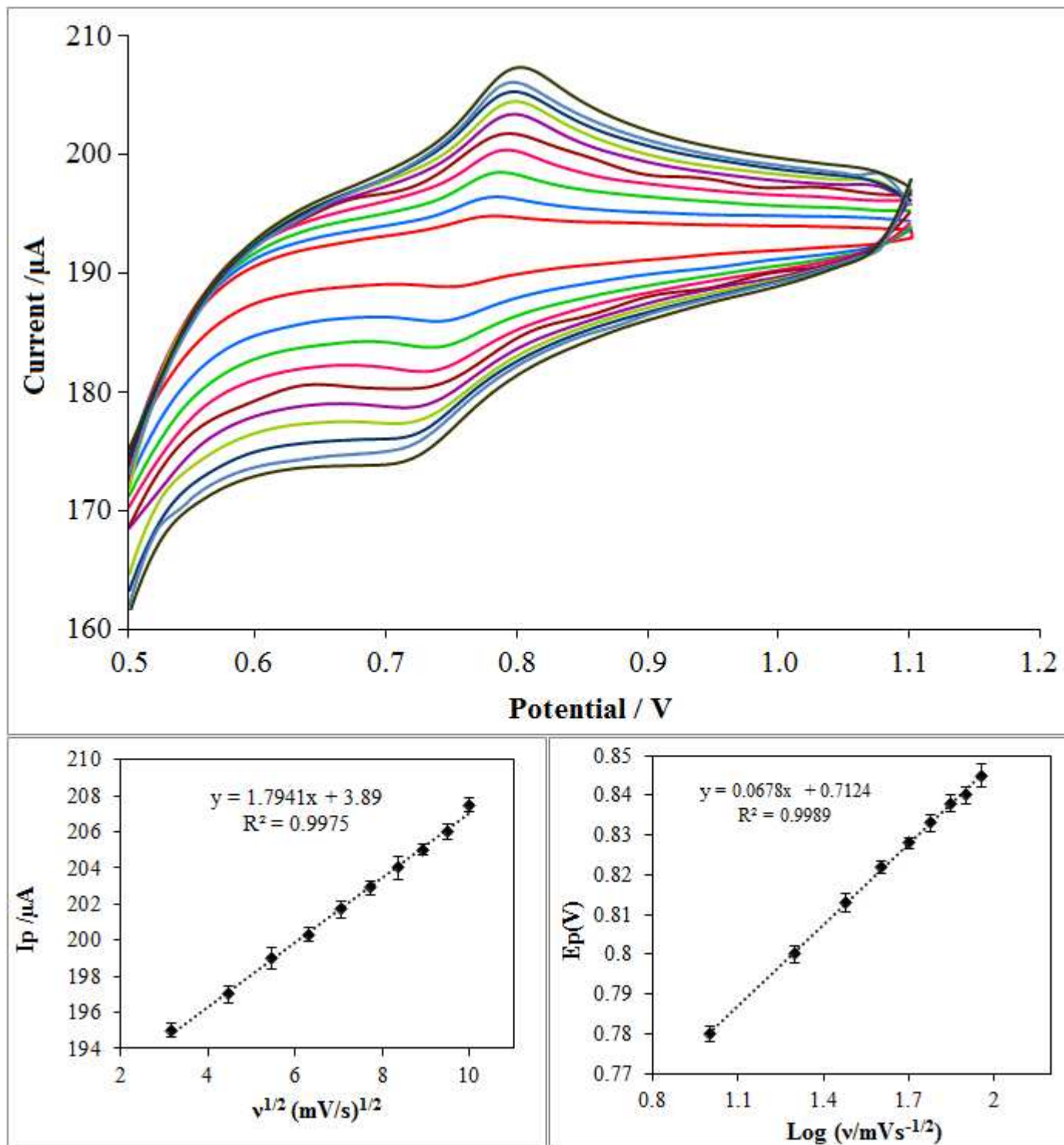


Fig. 7.

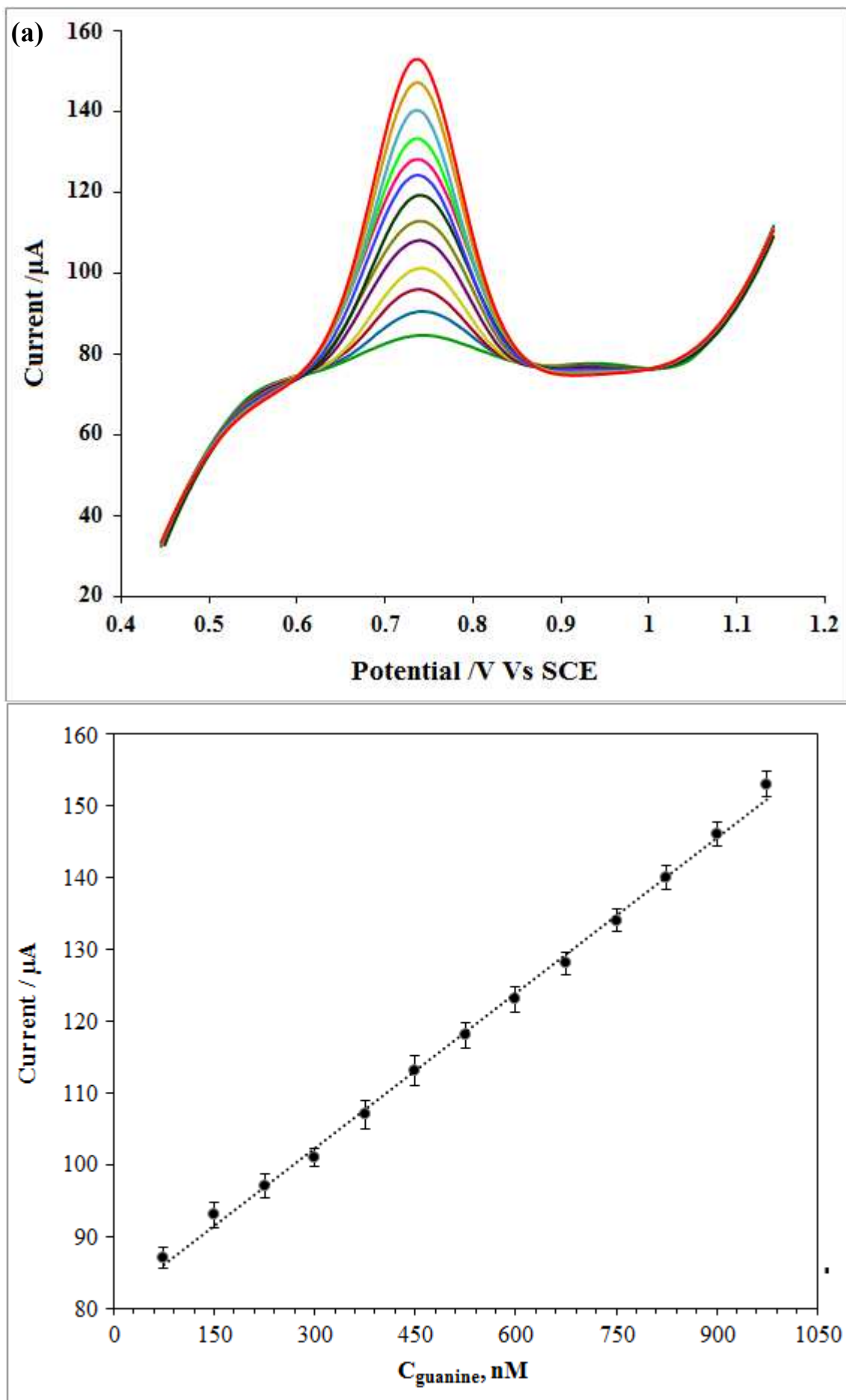




Fig. 8.

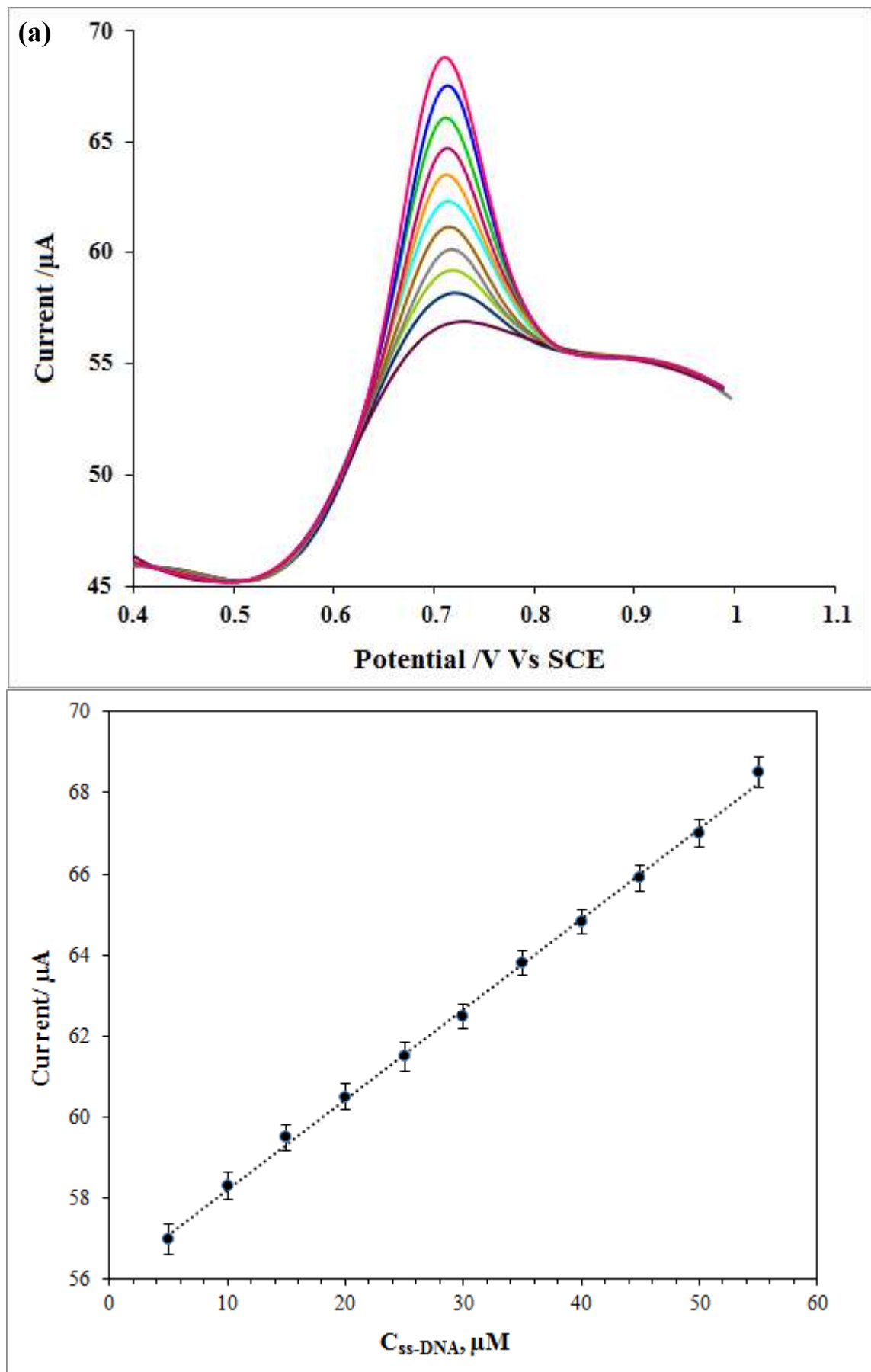


Fig. 9.

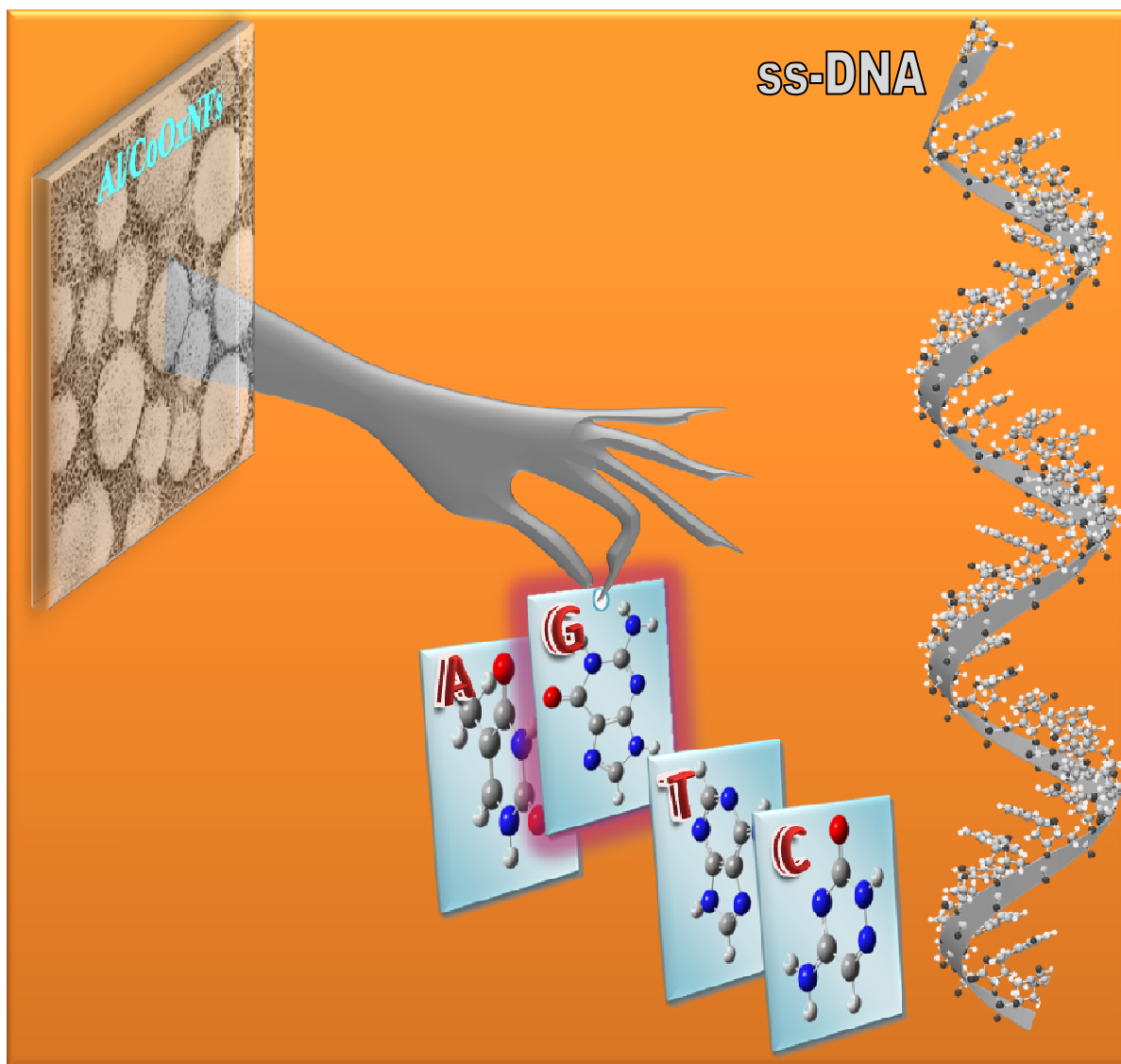
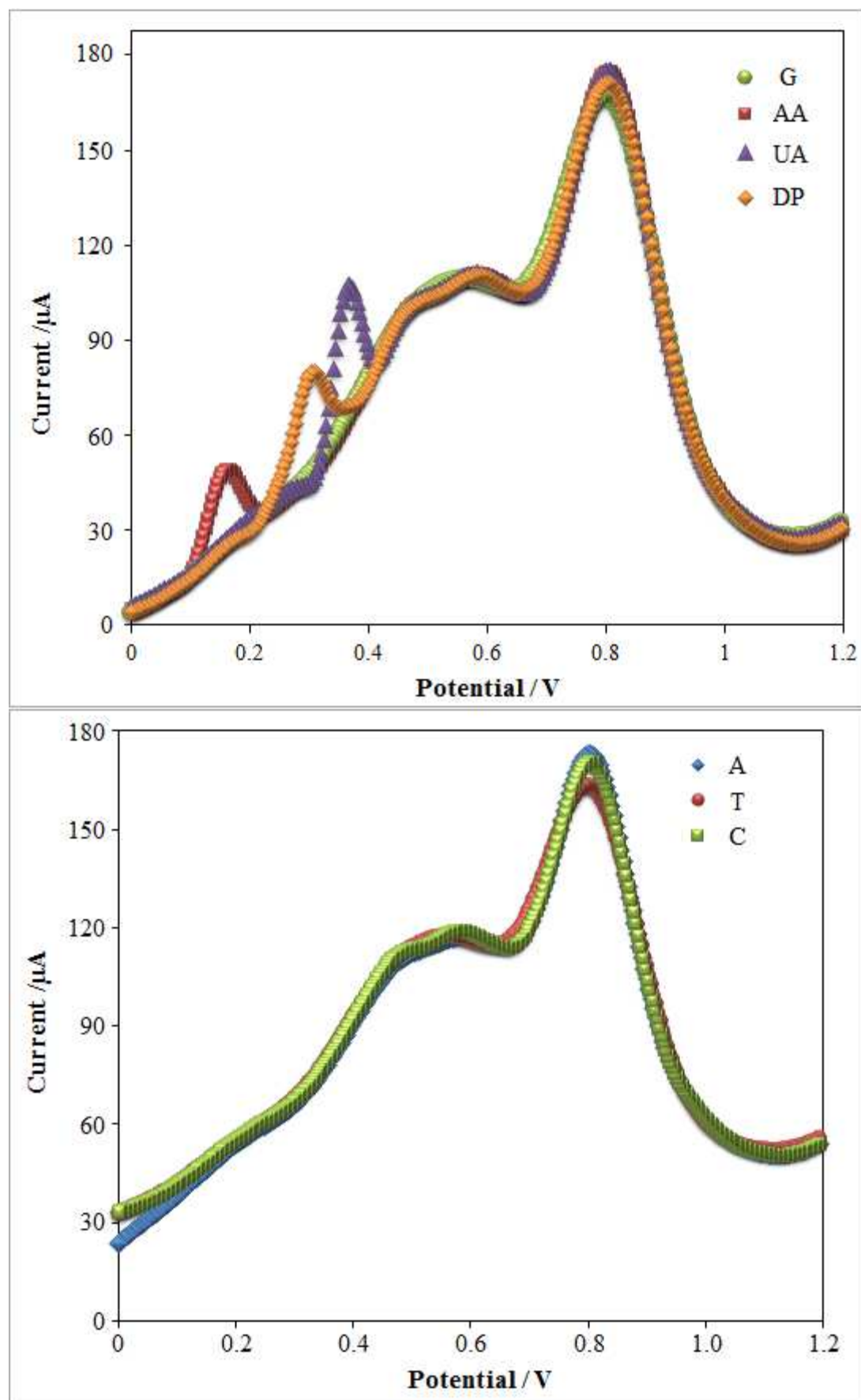
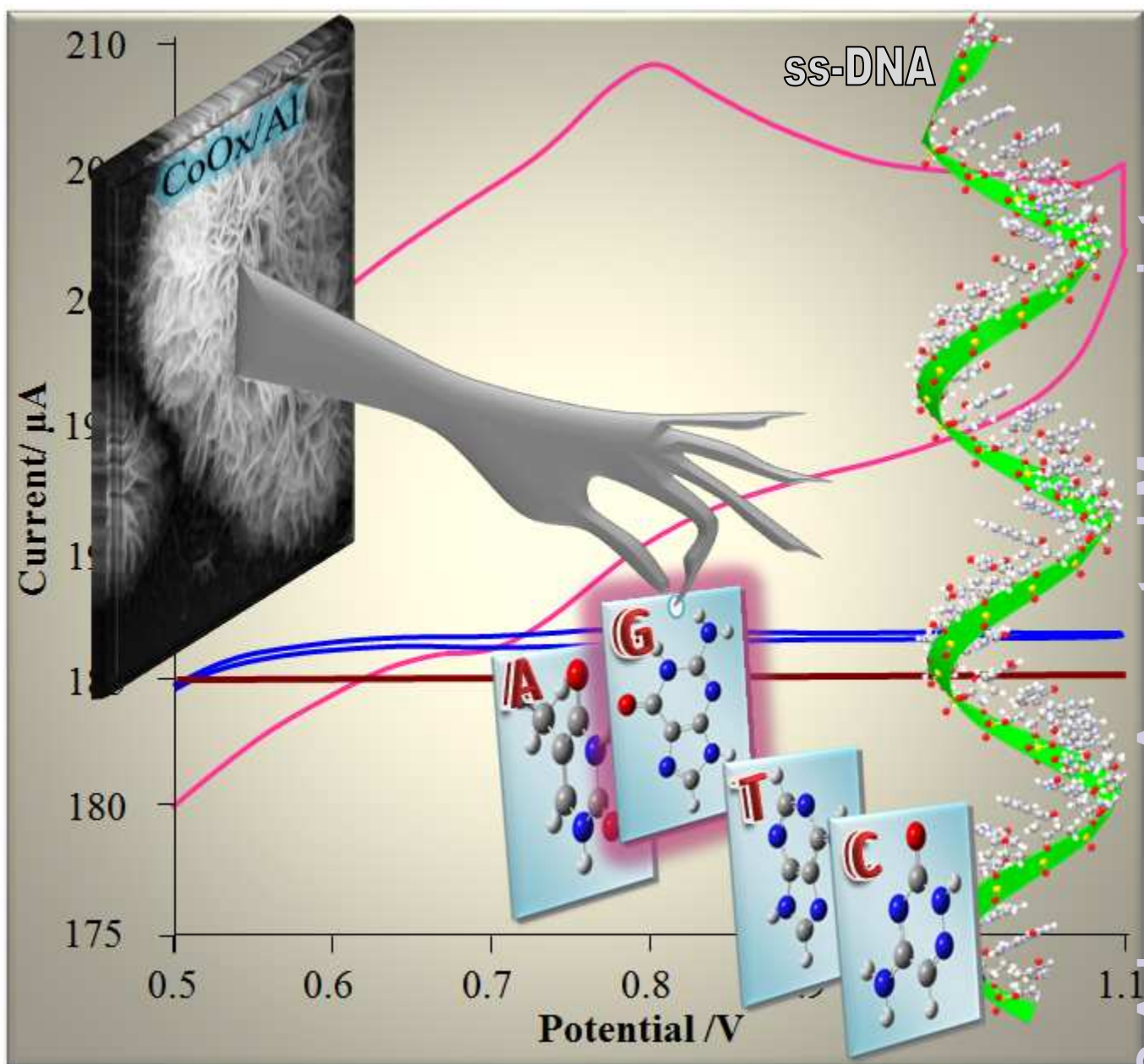


Fig. 10.



## Graphical Abstract



Electrocatalytic oxidation of guanine in ss-DNA at cobalt oxide nanoflower modified aluminium electrode